Bull. Nat. Inst. Oceanogr. & Fish., A.R.E. 1994. 20 (2): 29 - 54

THE INVESTIGATION OF THE PRINCIPAL SEMI-DIURNAL LUNAR TIDE AND TIDAL CURRENT IN THE GULF OF SUEZ USING A TWO DIMENSIONAL NUMERICAL MODEL.

By

G.F. SOLIMAN* AND H.A. ANWAR

***National Institute of Oceanography and Fisheries, Anfoushi, Alexandria, Egypt.**

Key Words: Physical Oceanography, Tidal Currents, Gulf of Suez, Red Sea.

ABSTRACT

The Two-dimensional hydrodynamical model of Hansen type (1956, 1962) that developed by Soliman et al (1993) has been modified to be applicable for shallow water regions. The modified model was used to investigate the principal semi-diurnal lunar tide in the Gulf of Suez. Grid systems of different grid dimensions have been considered. The influence of friction, boundaries, Coriolis force and islands barriers on the motion, were examined. The co-ranges, co-tidal lines and tidal currents, were presented. A rotating tidal motion exists in the Gulf as a degenerated amphidromy with a nodal point located on the western side of the Gulf in the vicinity of Ras Gharib. Strong currents, with speeds of more than 40.0 cm/sec, were traced in the area extended between Ras-Bakr and Ras Shukier, while relatively strong currents of speed more than 30.0 cm/sec, were found near Ashrafi. The co-ranges when neglecting the influence of the potential forces, are in good agreement with observations. Rotational motions (eddies) occurred at different locations during the transient motion, each has a cyclic or anticyclic character. The current ellipses are very clear in the southern part of the gulf with significant minor to major ratio which indicate the presence of transverse motion in that region. The tidal current patterns could be used to predict the total current.

INTRODUCTION

The Red Sea can be regarded as a long narrow basin with depths exceeding 2000m along its main axis. The sea is terminated at its northern end by two gulfs, the Gulf of Suez and Gulf of Aqaba. Based on the topographic characteristics of the sea, most investigators considered it as a deep canal(Harris, 1904; Blondel, 1912; Vercelli, 1925; Defant, 1926 and 1961; Sterneck, 1927; Chandon, 1930 and Grace, 1930), hence they ignored the influence of friction and the rotation of the earth. Soliman (1979) used a numerical model to investigate the M2-tide in the Red Sea but took into consideration the rotation of the earth and friction in its linear form. In his computations, the Gulf of Aqaba was ommitted while the Gulf of Suez was composed only of about eight grid points about 35.0 km apart, which are not enough to give in detail the sea water elevation at different locations.

Presently, both of the gulfs (Suez and Aqaba) have showed rapid developments in the infrastructure along their coasts which added new potential activities in the region besides the continuous investment of oil production. In order to wisely develop the coastal zone in the area, good information about sea level and water currents at the different regions, are required.

Although the two gulfs have nearly the same width, they showed wide variety in their bottom topography. While the Gulf of Suez (Fig.1) has nearly a flat bottom of about 60 m depth of its most region (except at its entrance where depths of more than 500 m exist), the gulf of Aqaba shows another type of bottom topography (resemble the Red Sea topography) where depths of more than 1000 m are found along its main axis. Thus, the two gulfs are considered as good examples for applying the hydrodynamical numerical models to investigate the tidal motion in two different basins; shallow and deep water basins. In the present study the first case of shallow water type has been considered.

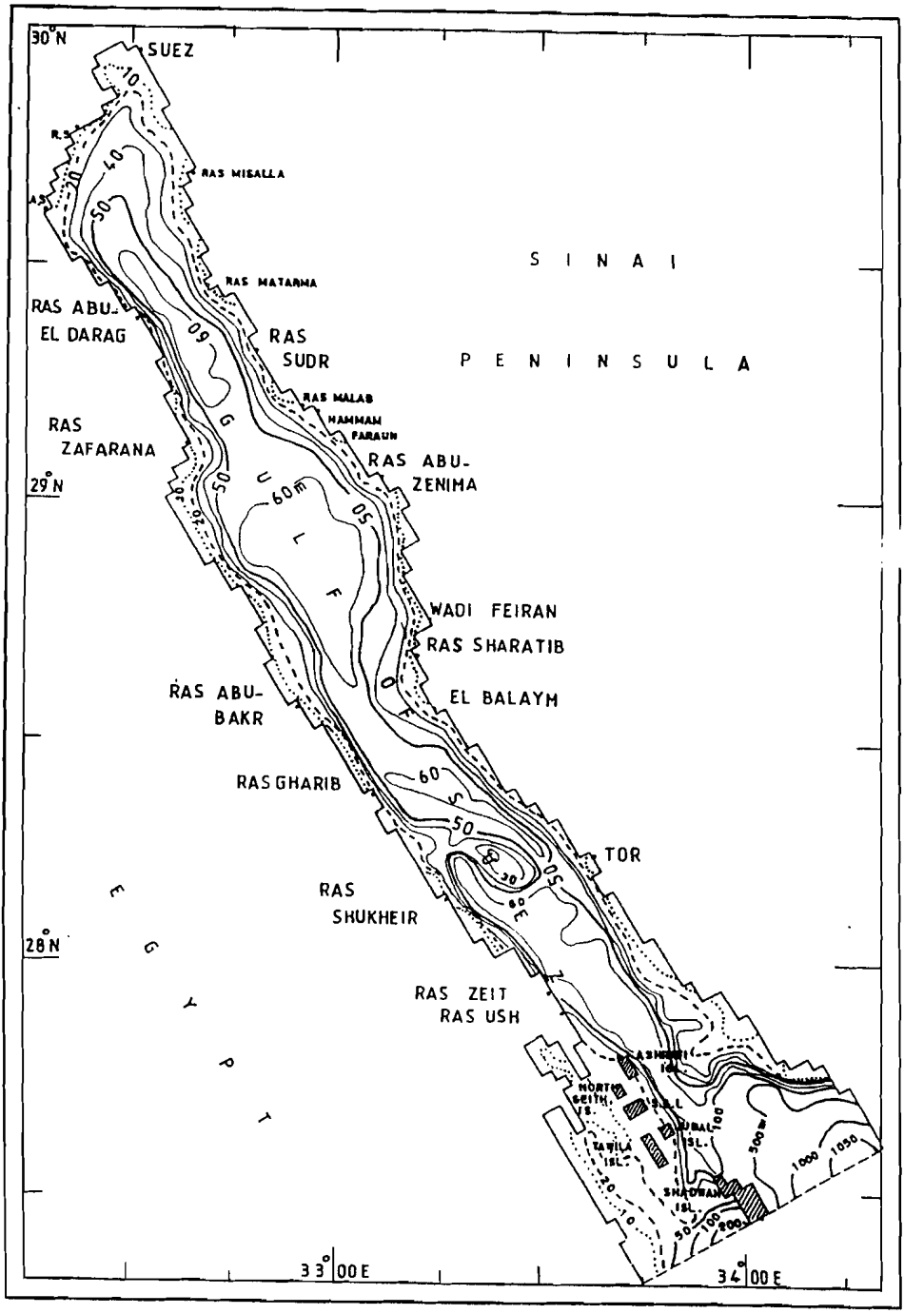

Fig. 1. Gulf of Suez Map.

The equations of motion and the numerical model

A two dimensional model of Hansen type (1956 and 1962) that developed by Soliman et al (1993) has been modified. The vertically integrated hydrodynamical differential equations were taken as follows:

$$\delta u/\delta t - fv + \tau^b_x + g\,\delta\,\xi\,/\delta x - X = 0 \quad \ldots\ldots\ (1)$$

$$\delta v/\delta t + fu + \tau^b_y + g\,\delta\,\xi/\delta y - Y = 0 \quad \ldots\ldots\ (2)$$

$$\delta\,\xi/\delta t + \delta(Hu)/\delta x + \delta(Hv)/\delta y = 0 \quad \ldots\ldots\ (3)$$

where:

- x,y : cartesian co-ordinates in the northwest and northeast directions respectively resulted from the rotation of the axis 30° to the left,
- t : time,
- ξ : water elevation of the free surface,
- u,v : components of the depth mean current in the new x- and y-directions respectively,
- H : total water depth,
- f : Coriolis parameter,
- τ^b_x , τ^b_y : components of frictional forces at the bottom in the new x-&y- directions respectively,
- g : acceleration due to gravity,
- X,Y : components of the tide-producing force in the new x- & y- directions respectively.

Initial and boundary conditions

The free surface was assumed as a function of x (sinusoidal shape) at t=o, i.e.:

$$\xi = 25.0 \cos \pi[(I-1)/117] \quad \ldots\ldots\ (4)$$

$$\& \quad u = v = o \quad \text{everywhere} \quad \ldots\ldots\ (5)$$

where:

I,J : grid numbers in x-and y-directions respectively.

The normal component of the depth mean current has to vanish at the boundaries.

$$\text{i.e. } v_n = o \quad \text{at } H = 0 \quad \ldots\ldots\ (6)$$

Frictional forces

Quadratic frictional type was found to be appropriate in shallow water areas. Its components in the x- and y- directions were estimated using the following relationships:

$$\tau^b_x = R\, u\, (u^2 + v^2)^{1/2} / (H + \xi) \quad \ldots\ldots\ldots\ldots \quad (7)$$

$$\tau^b_y = R\, v\, ((u^2 + v^2)^{1/2} / (H + \xi) \quad \ldots\ldots\ldots\ldots \quad (8)$$

where:

R : coefficient of friction $\simeq 5 * 10\text{-}^3$

Grid system

The grid system was constructed as shown in Fig.2. At each grid point, u-points (*) exist on the y-directed sides, v-points (+) on the x-directed sides and ξ -points (.) at the middle of the grid. A grid system of fine resolution of dimensions : x = 2.78 km, y = 2.44 km was constructed. The basic array comprises , 117 x 28 = 3276 points with I = 117 and J = 28.

The difference scheme

A simple explicit finite difference scheme was set to estimate ζ(i,j,t +Δ t), u (i,j,t +Δ t) and v (i,j,t +Δ t) at time t + Δ t from the known values already computed at time t with forward time difference and central differences for space derivatives.

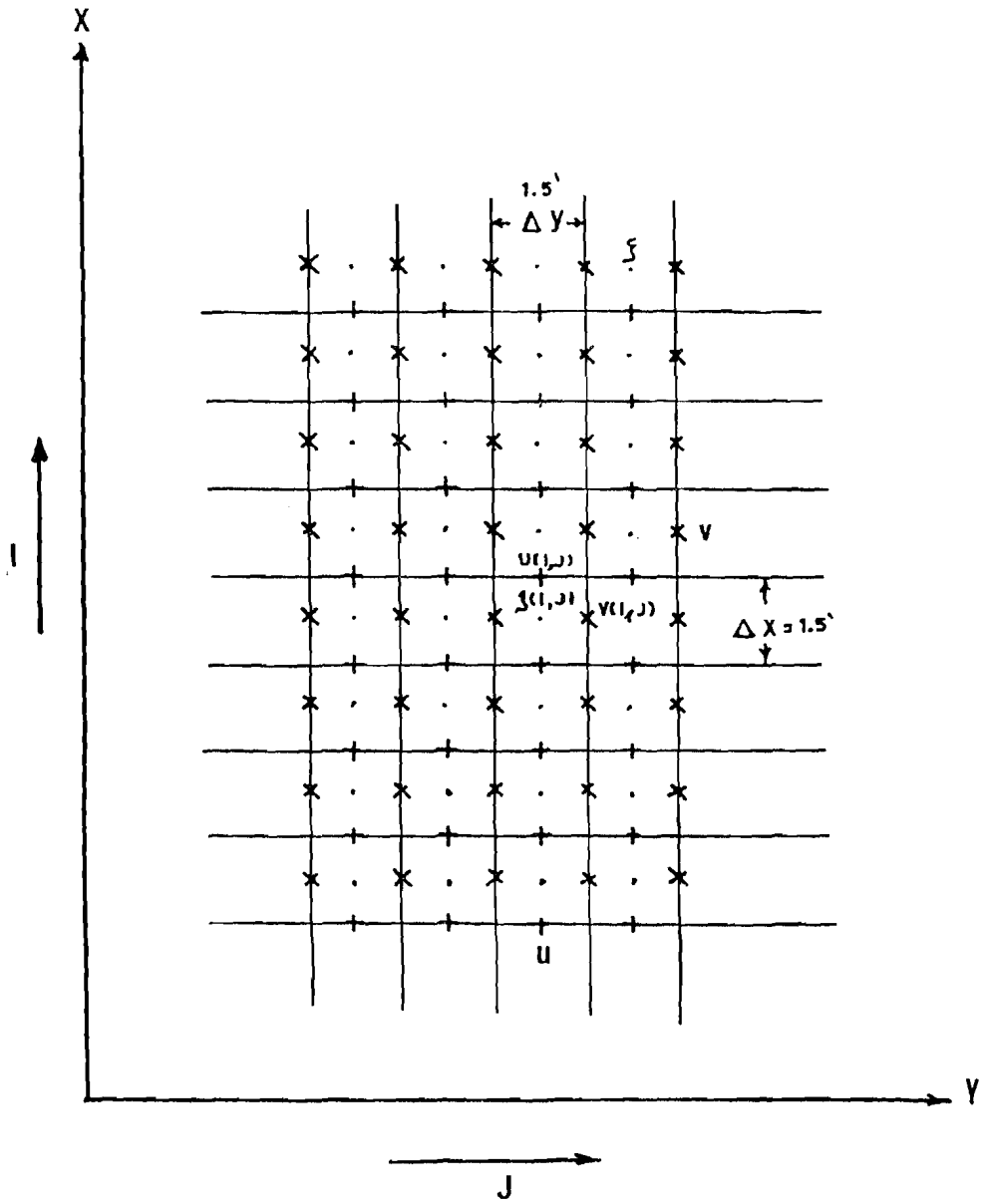

Fig. 2. The grid system used in the numerical computation with the positioning of -, u-, and v- points.

At a ξ -point, when $\delta u/\delta x$ and $\delta v/\delta y$ are required to be calculated the central difference approximation is used as:

$$\Delta_x u = u(i,j) - u(i-1,j)$$
$$\Delta_y v = v(i,j) - v(i,j-1) \quad \ldots\ldots\ldots (9)$$

Similarly, at a u-point and a v-point, Δ_x^{ξ} and Δ_y^{ξ} are obtained.

In the case of computing the Coriolis force, the values of v are required to be evaluated at u- points and the values of u at v-points through space averaging within a single lattice (Platzman, 1972) as a weighted mean, with the weight q given by the ratio:

$$q = f/H \quad \ldots\ldots\ldots\ldots\ldots\ldots\ldots\ldots (10)$$

therefore, space average of $v = 0.25 * q_o^{-1} * [\sum_{k=1}^{4} 0.5*(q_o+q_k)\ v_k] \ldots\ldots\ldots\ldots\ldots\ldots (11)$

where

q_o is the weight at u-point. The same thing is obtained for the space average of u.

Stability conditions

The stability criteria of a simple wave (Friedriches-Lewy Criterian) is given by :

$$\Delta t \leq \Delta x/(2g H_{max})^{1/2} \qquad \text{for } f = 0 \ldots\ldots\ldots (12)$$

and

$$\Delta t \leq R / Hf^2 \qquad \text{for } f \neq 0 \ldots\ldots\ldots (13)$$

Stability conditions reached after computation of three tidal cycles.

RESULTS AND DISCUSSION

Since the work of Vercelli (1925), Defant (1926), Sterneck (1927) and Grace '30) on the tides of the Red Sea and both Gulfs of Suez and Aqaba, no further orks have been carried out on these regions till the recent work of Soliman (1979),

Soliman and Gerges (1983) and Rady (1992). Although the Gulf of Suez is simple in its shape and relatively shallow in depth, the theoretical investigation of its tides is still unsatisfactory.

The disagreement between calculations and observations of the tidal constants in the Suez Gulf particularly in the northern part of the gulf could not be overcome by different investigators and was explained by Grace (1930) as a result of ignoring the transverse motions and friction which were regarded by him to be more disturbing there.

Recently, Rady (1992) used a non-linear barotropic two-dimensional model to estimate M2-co-oscillating tide in the Gulf of Suez. A degenerated amphidromic point was observed to the west. He showed that the tidal currents of the southern sector (60-80 cm/sec) are much stronger than those of the northern sector (5-20 cm/sec). A good agreement is found between computed and observed amplitudes except near the boundary. He attributed these deviations to the model formulation which does not allow the reflected waves to leave the model. Moreover, he applied a three-dimensional model to the same area, and concluded that the agreement between the observed and computed tides is much better in the two-dimensional than in the three-dimensional simulation. In addition, the gyratory anticlock wise motion in the top three layers during slack water following the flood tide does not appear in the two-dimensional simulation.

Defant (1926) and Sterneck (1927) showed that tides in the northern and southern parts of the Gulf of Suez are of semi-diurnal type. They added, semi-diurnal nodal line appears in the vicinity of Tor Bank and the tides there are of a mixed character. Sterneck (1927) noted also that an amphidromy of contra solem character seems to exist in the region.

The results of the present study as shown in Fig.(3a-c) gives the co-ranges (in cm) and the co-tidal lines (in lunar hours) on a rotating earth with friction coefficient of $5 * 10^{-3}$ and grid system of dimensions : x = 5.559 km, y =4.878 km (I= 60, J=14). The co-ranges, if completed on both sides seem like ellipses around a nodal point existing on the western side of the gulf in the vicinity of Ras Shukier where the co-tidal lines appear as a degenerated amphidromy rotating in an anti-clock wise direction. Hence, it is concluded that, the M2-tidal motion in the Gulf of Suez is not

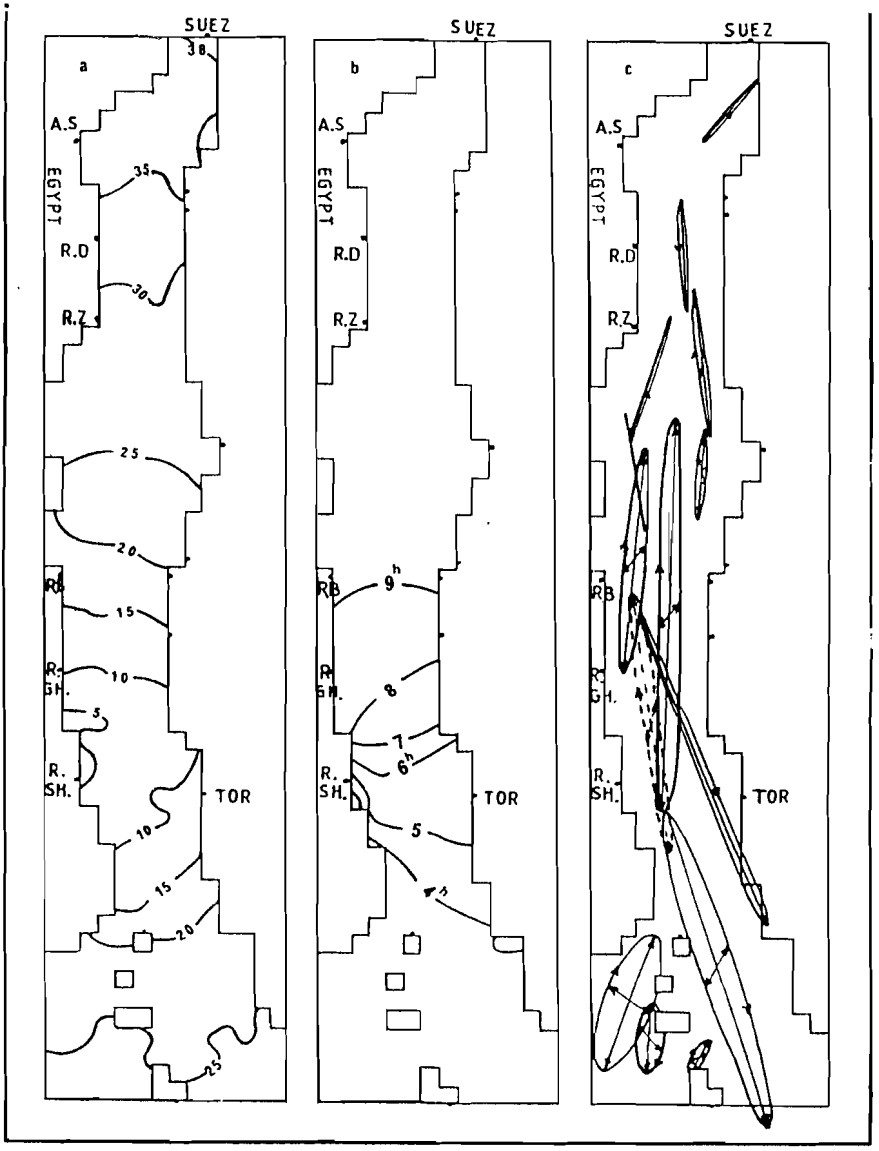

Fig. 3 M2-co-oscillating tide in the Gulf of Suez (with grid size 3' * 3') with its real depths and friction coefficient of 5 * 10-³.
a) The co-ranges in cm., b) the co-tidal lines in lunar hours at high tide after lunar-transit at Greenwich .
c) Current ellipses at different points in the gulf.

a simple longitudinal standing wave, but it appears as a Kelvin wave. The incident wave seems to be reflected at the head of the gulf in the north, resulting in the formation of a degenerated amphidromy.

The results showed also that mostly, the northern half of the gulf has nearly the same phase angle which indicates that the water rises and falls gradually overall the region at the same time. In addition, high water occurs in the north when low water is existing in the south and vice versa.

Fig. 4 presents the spatial distribution of depth mean current of the M2-co-oscillating tide at intervals of three lunar hours. The current patterns indicate the occurrence of ebb currents in the north (southward currents) as the water starts to fall at Suez, and flood currents (northward currents) as the water starts to rise there. Maximum ebb and flood currents occur during the transient time. Strong currents nearly appear at the middle part of the gulf in the vicinity of Ras Gharib where the speed exceeds 30.0 cm/sec. Relatively weak currents of about 22.0 cm/sec were observed at Ashrafi. Variations in the width and the depth of the gulf have great influences on the speed and direction of the current. Reflections and refraction of the tidal waves could then be easily traced along the length of the gulf. In addition, on approaching from high or low tides, eddies of different types of rotation are taking-place (Figs. 4 b & 4 d) at different locations. These are very important feature in the marine environment.

The current ellipses are given at certain grid points (Fig.3c). The influence of the transverse motion appears quite well in the southern part of the gulf, where the ratio between minor and major axes is significant .

Using finer grid resolution (x =2.78 km, y=2.44 km) more precise results were obtained for different conditions. Different conditions of water depths, Coriolis force, existence natural barriers as islands in the south and potential forces were considered.

Figs. 5-9 present the co-ranges (in cm) and co-tidal lines (in lunar hours) on applying the two dimensional model with friction coefficient of 5 * 10^{-3} on the Gulf of Suez for the foregoing conditions: the real depths distribution H(I,J) as given in the Admiralty chart; the depths distribution after correction to the mean sea level; the same condition of the last depths distribution on a non-rotating earth (i.e. f=o); also the same depths distribution but replacing the islands in the south with water of about 5.0 m deep and hence finally the last foresighted condition but ignoring the influence of the potential forces (i.e. X = Y = o). The computed values of amplitudes and phase angles are greatly improved in comparison with either the calculated results obtained from using the grid system with dimensions x = 5.559 km and y = 4.878 km., or the previous theoretical results obtained by Defant and Sterneck (Table 1). Comparing the results of the present model with field observations, it can be seen that the present results are in good agreement .

Fig. 10 illustrates the tidal current as obtained for real bottom topography after correcting it to the mean sea level. While Fig. 11 gives the tidal current on a non-rotating earth. Thus we can test the influence of the earth's rotation and the accompanied transverse motions on the current pattern. The model indicates that the currents are relatively stronger and more developed particularly in the near-shore areas.

In 1923 the Italian Expedition AMMIRAGLIO MAGNAGHI (Vercelli, 1925) has obtained current measurements for about 1-1.5 day at three locations : At Zafarana (about 15.0 cm/sec), Ras Mallap east of Zafarana (20.0 cm/sec) and on Tor Bank (40.0 cm/sec). New observations were recorded in 1981 at the entrance of the gulf on board Karam El-Suez (Roberts and Murray, 1984; Soliman, in preparation). The computational results of current are also in good agreement with observations. The current ellipses were presented at different location (Fig. 12).

Table (1): Amplitudes (in cm) and phases (in degrees of high tide after lunar transit at Greenwich) of observed and computed M2-tide in the Gulf of Suez.

Values / Location	Observed values			Calculated Values																	
				Previous Works						Present Work											
				Defant (1926)* M2+S2		Soliman (1979) as long Canal		Soliman (1979)** Two dimensional		Grid dimension 5.56 * 4.88 Km		Grid dimension 2.78 * 2.44 Km		Grid dimension 2.78 * 2.44 Km		Grid dimension 2.78 * 2.44 Km		Grid dimension 2.78 * 2.44 Km		Grid dimension 2.78 * 2 44 Km	
	A	ϕ	ϕ	A	ϕ	A	ϕ	A	ϕ	A	ϕ	A	ϕ	A	ϕ	A	ϕ	A	ϕ	A	ϕ
	(Cm)	at Aden	at Greenw.	(cm)	o	(cm)	o	(cm)	o	(Cm)	o	(Cm)	o	(Cm)	o	(Cm)	o	(Cm)	o	(Cm)	o
Suez	56.1	342	290 (278)	61 (70)	296	56	260	41	292	39.2	284	45.7	278	46.8	278	45.9	279	47.5	277	49	277
Zafrana	42.4	345	289 (280)	50 (55.1)	296	41.1	255	28	287	29	282	35.8	280	36.2	280	35.4	278	37	278	38.1	279
Ras Gharib	18.2	340	288 (274)	12 (25.2)	292	13.6	247	8	274	11.2	268	13.1	264	14.4	266	14.6	261	14.8	264	15.4	266
Tor	7.8	271	216 (203)	9 (9.7)	126	11.5	154	3.3	200	12.2	177	8.5	165	8.2	170	6.3	165	8.3	172	8.2	175
Ashrafi	13.4	184	131 (116)	23 (17.4)	126	18.7	129	14.8	130	15.9	127	14.8	121	14.6	119	15.1	125	15	117	15	117
Shadwan	25.1	185	130 (117)	29 (27.4)	122	22.6	106	20.5	127	25.4	123	25.4	120	25.4	120	25.4	120	25.4	120	25.4	120

* Amplitudes between ( ) correspond to observations of M2 + S2

** The Gulf of Suez itself was a one dimensional basin of 8 grid - points along its length and one grid point in width.

1- with real depths.
2- with real depths refered to the mean sea level
3- " " " " " " " " " and non-rotating earth.
4- " " " " " " " " " and ignoring the islands.
5- " " " " " " " " " and ignoring the tide producing forces.

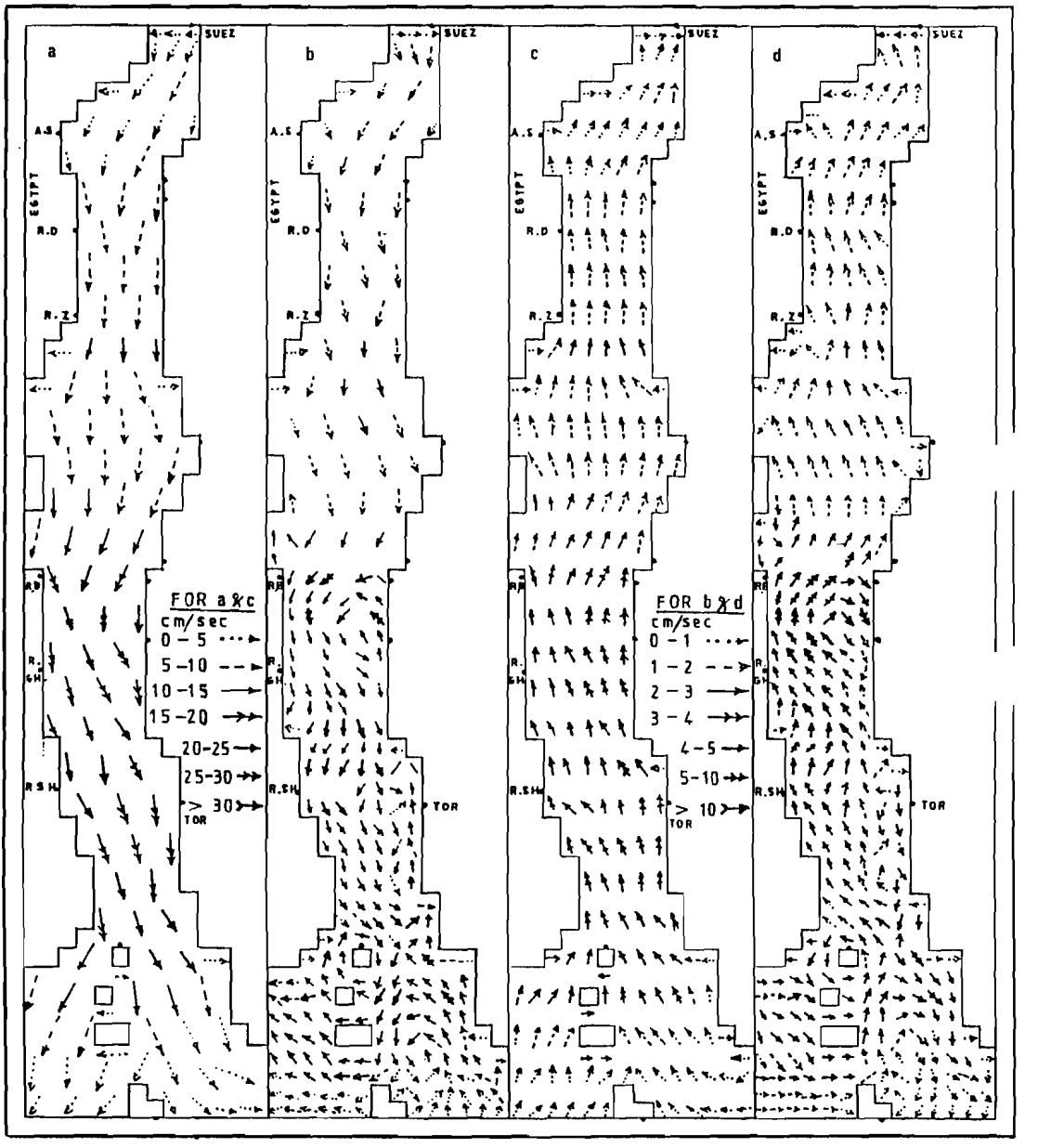

Fig. 4 The spatial distribution of depth mean current of the M2-co-oscillating tide (with grid size 3'*3') at intervals of three lunar hours (0,3,6 and 9h).

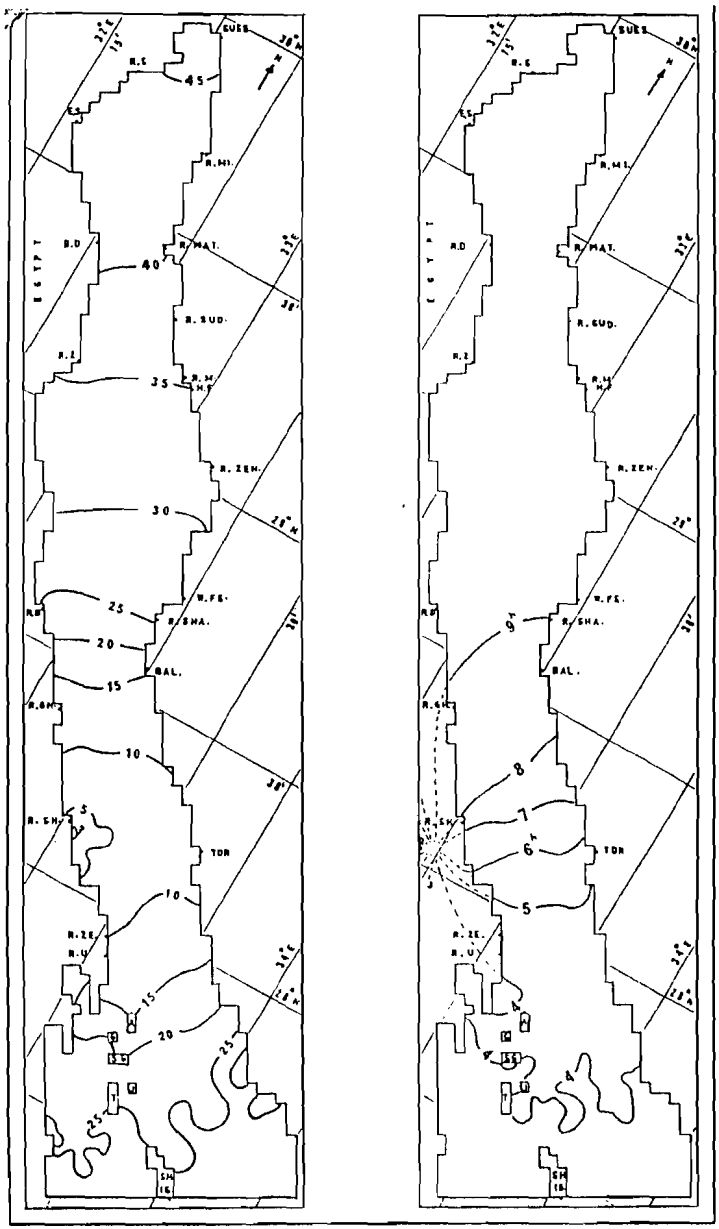

Fig. 5. M2-co-oscillating tide in the Gulf of Suez (with grid size 1.5' * 1.5') with its real depths and friction coefficient of 5 * 10^{-3}.
The co-ranges are in cm.(left), and the co-tidal lines in lunar hours at high tide after lunar-transit at Greenwich (right).

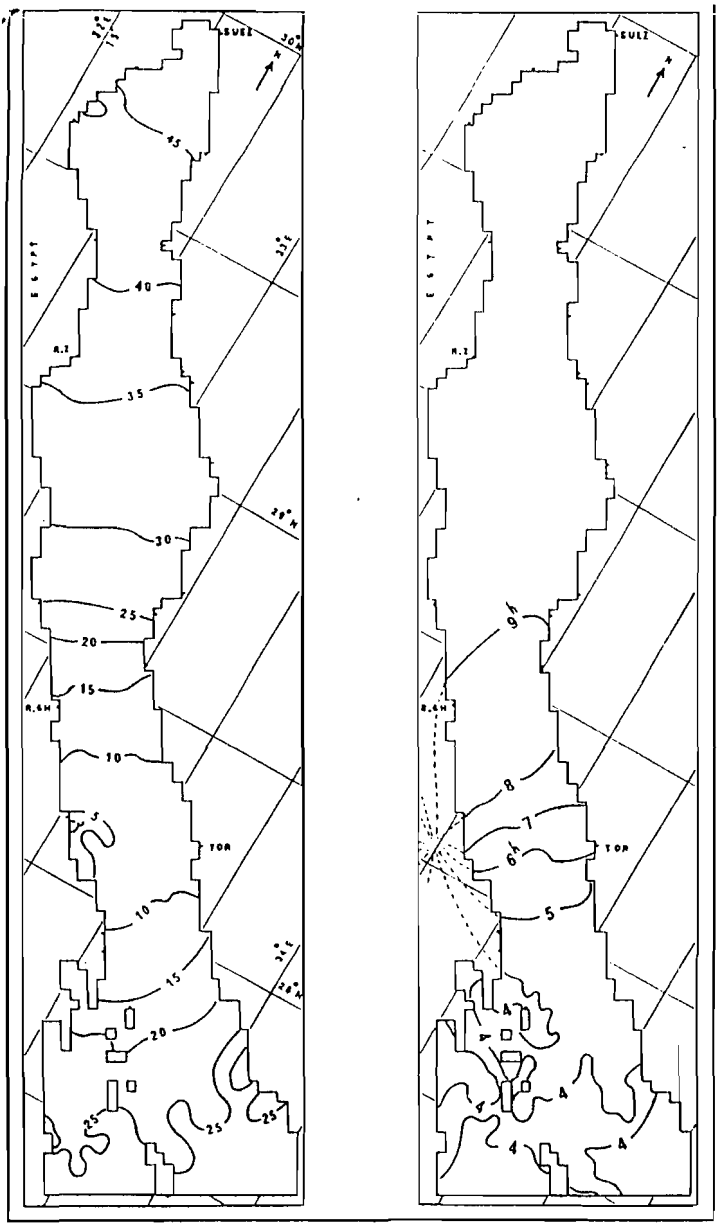

Fig. 6. M2-co-oscillating tide in the Gulf of Suez (with grid size 1.5' * 1.5') with its real depths refered to the mean sea level and friction coefficient of 5 * 10^{-3}. The co-ranges are in cm.(left), and the co-tidal lines in lunar hours at high tide after lunar-transit at Greenwich (right).

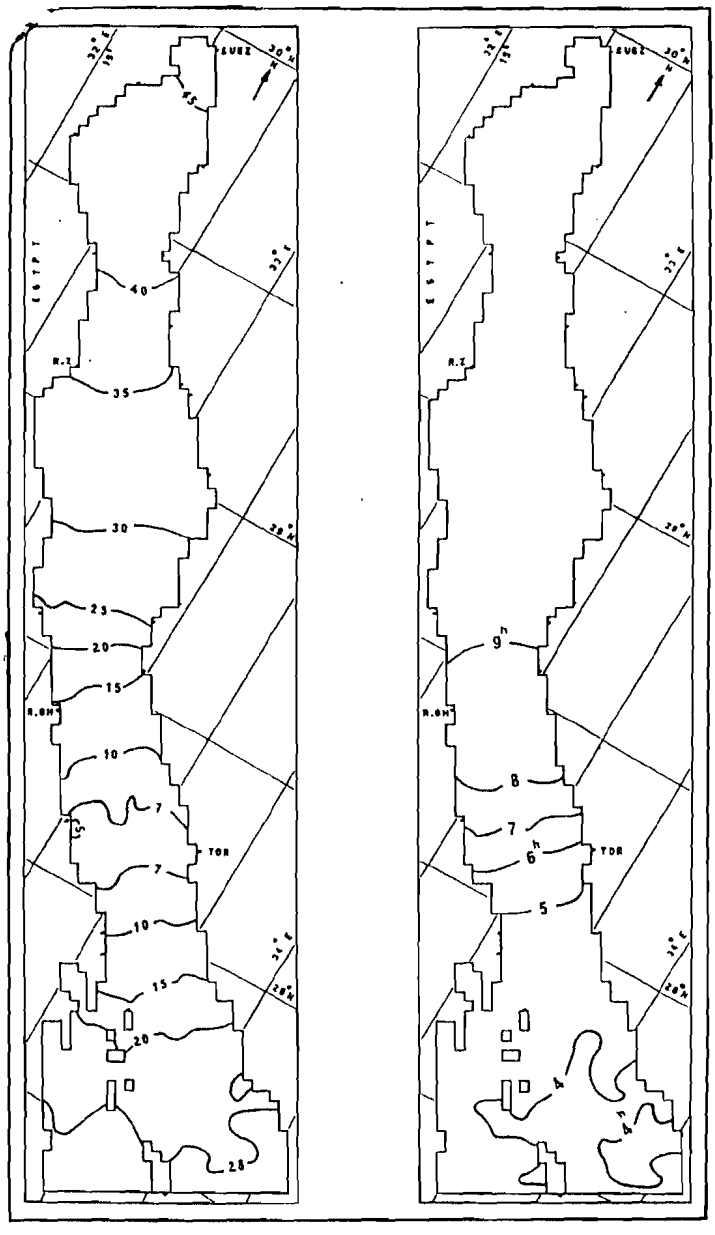

Fig. 7. M2-co-oscillating tide on a non-rotating earth (i.e.f=0) in the Gulf of Suez (with grid size 1.5' * 1.5') with its real depths refered to the mean sea level and friction coefficient of 5 * 10^{-3}. The co-ranges are in cm.(left), and the co-tidal lines in lunar hours at high tide after lunar-transit a Greenwich (right).

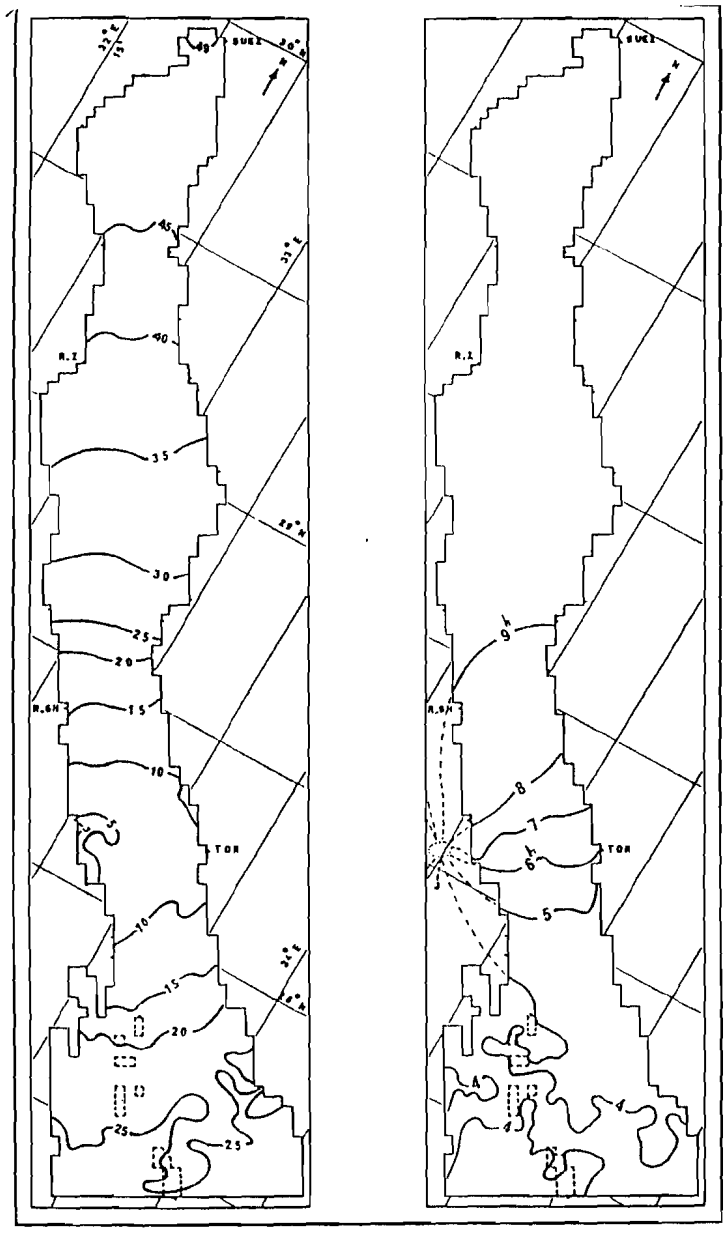

Fig. 8. M2-co-oscillating tide in the Gulf of Suez (with grid size 1.5' * 1.5') with its real depths refered to the mean sea level and friction coefficient of 5 * 10^{-3}. The islands have been ignored and replaced by water of 5m depth. The co-ranges are in cm.(left), and the co -tidal lines in lunar hours at high tide after lunar -transit at Greenwich (right).

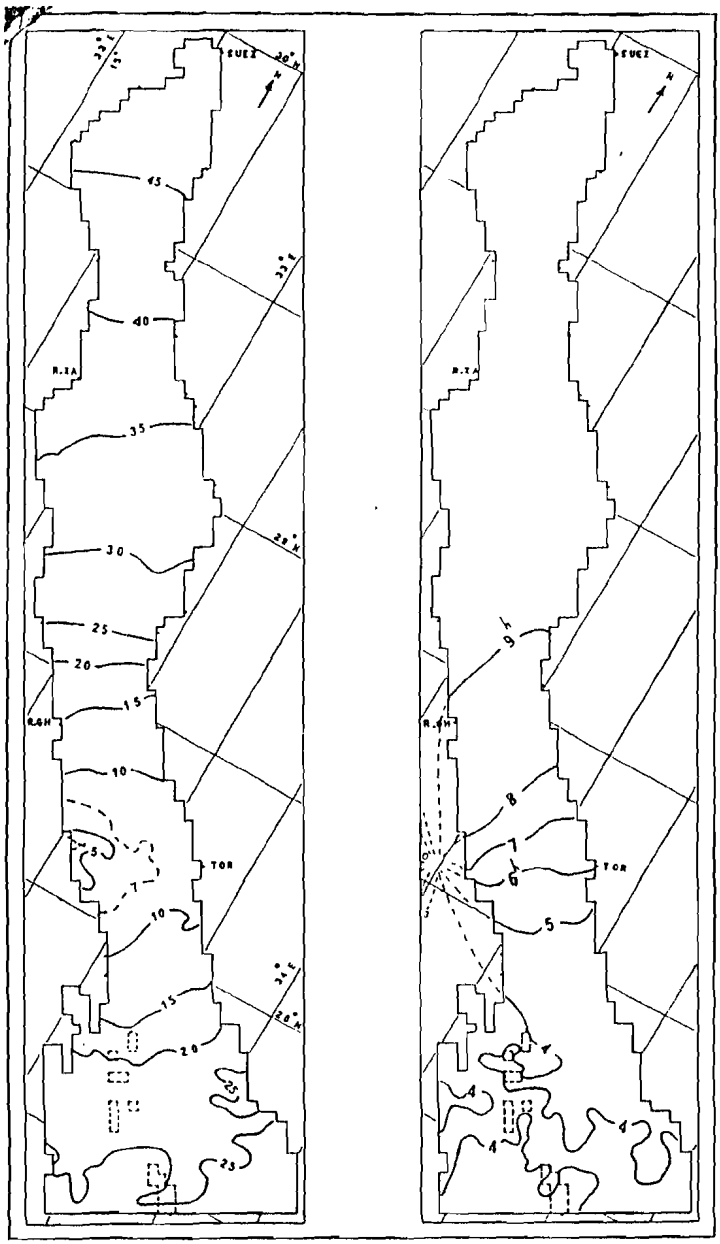

Figure 9: M2-co-oscillating tide (due only to the co-oscillation of the gulf with the Red Sea, i.e. X=Y=0) in the Gulf of Suez (with grid size 1.5'*1.5') with its real depths refered to the mean sea level and friction coefficient of $5*10^{-3}$. The islands have been ignored and replaced by water of 5m depth. The co-ranges are in cm.(left), and the co-tidal lines in lunar hours at high tide after luna-transit at Greenwich (right).

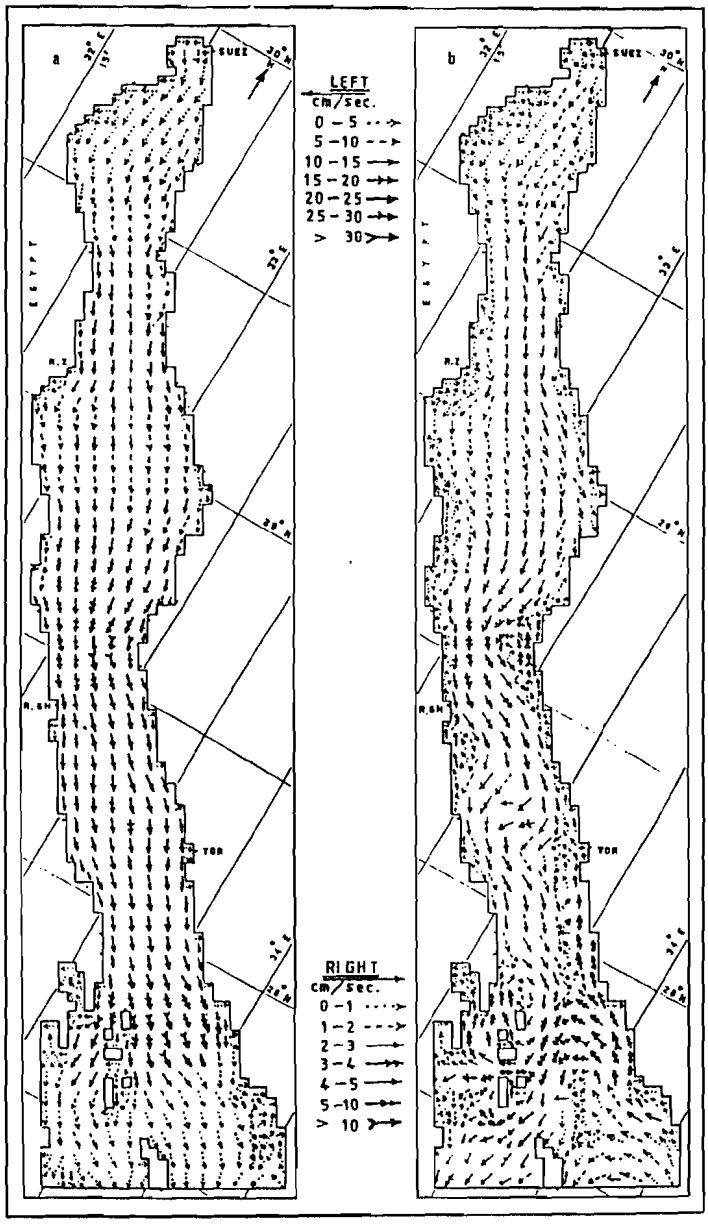

Figure 10 a-b: The spatial distribution of depth mean current of the M2-co-oscillating tide (with grid size 1.5'*1.5' with its real depths refered to the mean sea level at intervals of three lunar hours (0,3,6 and 9h).

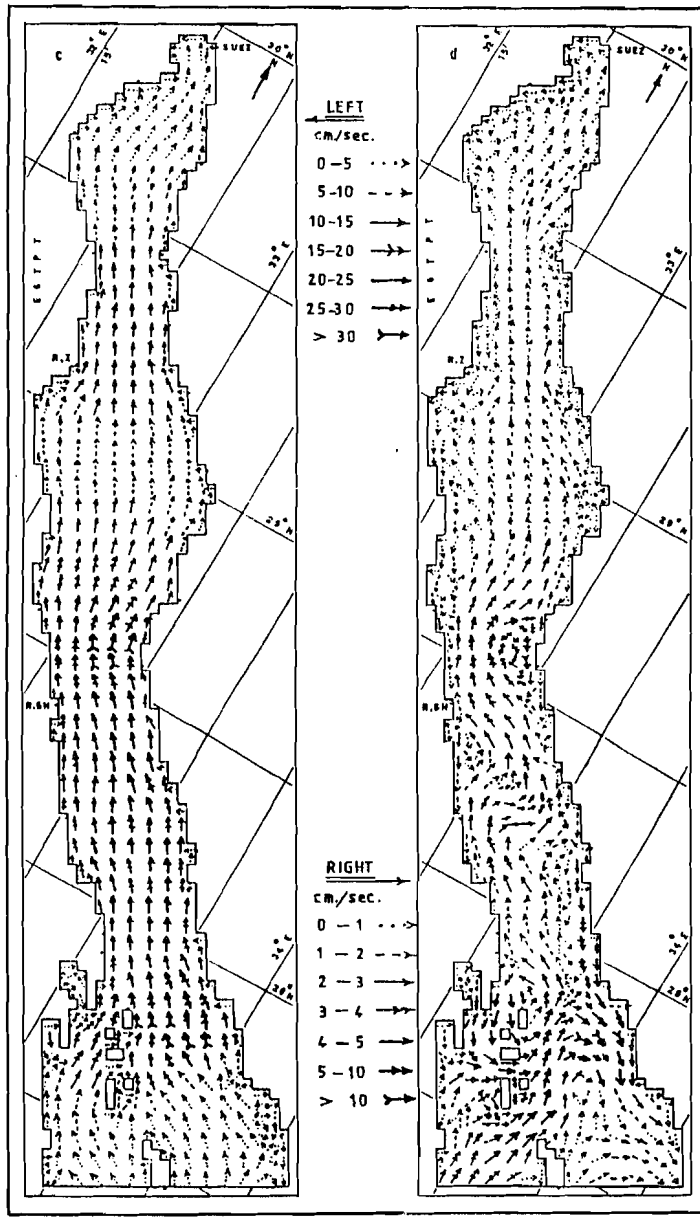

Figure 10 c-d: The spatial distribution of depth mean current of the M2-co-oscillating tide (with grid size 1.5'*1.5' with its real depths refered to the mean sea level at intervals of three lunar hours (0,3,6 and 9h).

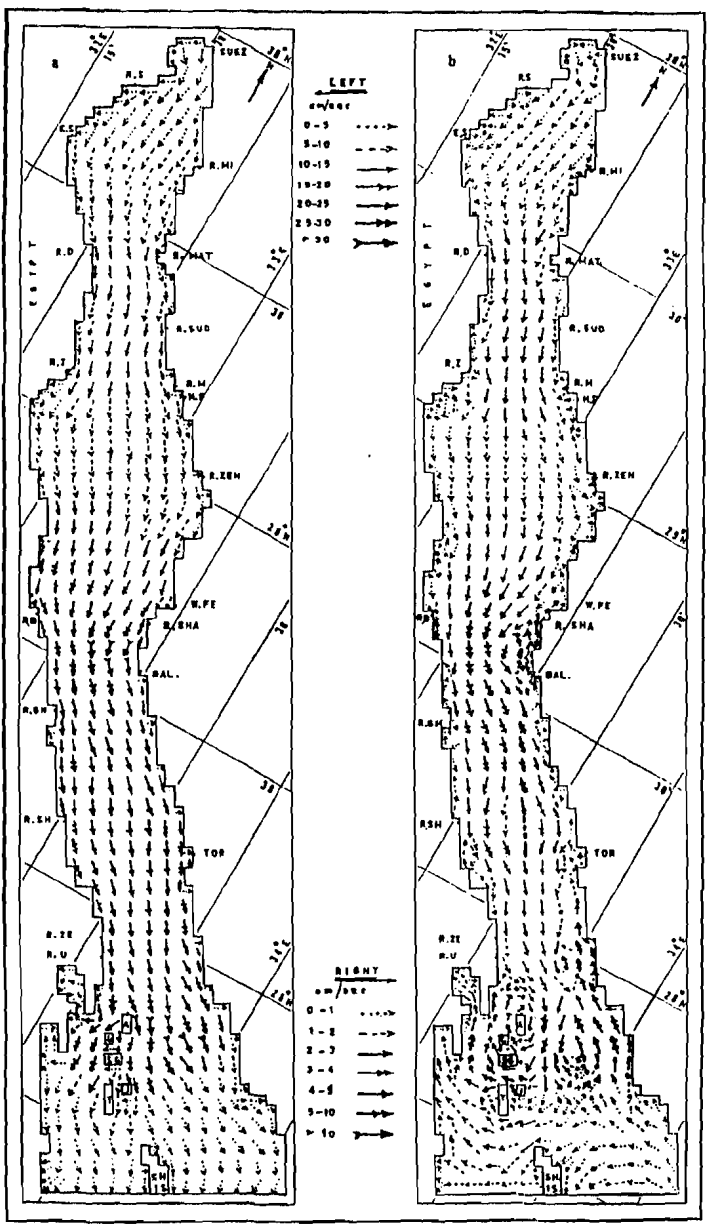

Figure 11 a-b: The spatial distribution of depth mean current on a non-rotating earth (i.e.f=0) of the M2-co-oscillating tide (with grid size 1.5'*1.5') with its real depths refered to the mean sea level at intervals of three lunar hours (0,3,6 and 9h).

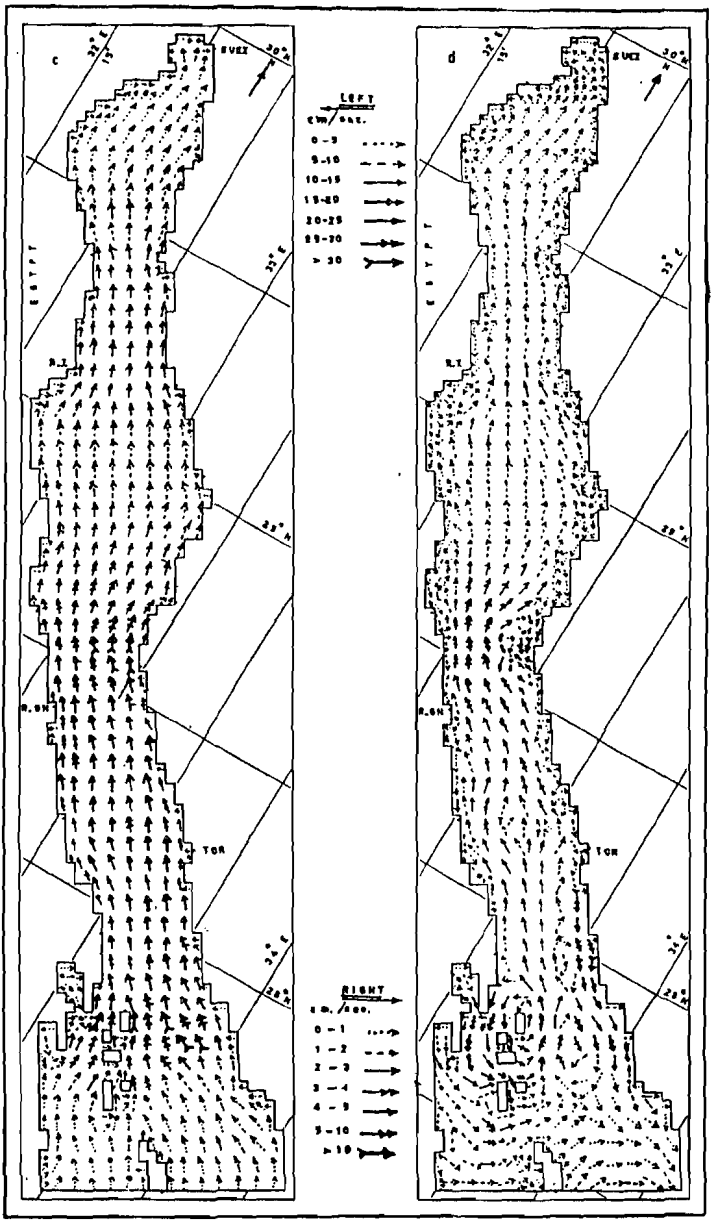

Figure 11 c-d: The spatial distribution of depth mean current on a non-rotating earth (i.e.f=0) of the M2-co-oscillating tide (with grid size 1.5'*1.5') with its real depths refered to the mean sea level at intervals of three lunar hours (0,3,6 and 9h).

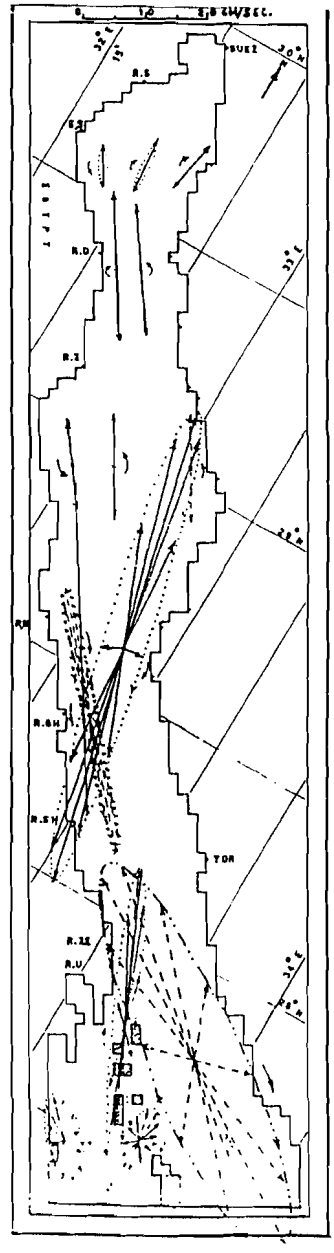

Fig. 12. Current ellipses at different points in the Gulf of Suez (with grid size 1.5'*1.5') with its real depth refered to the mean sea level.

CONCLUSION

1- The M2-tidal motion in the Gulf of Suez is not a simple longitudinal standing wave, but it appears as a Kelvin wave. The incident wave seems to be reflected at the head of the gulf in the north, resulting in the formation of a degenerated amphidromy. The nodal point is viewed on the western side of the gulf.

2- Most of the northern part of the gulf exhibits nearly the same phase angle, which indicates that the water rises and falls gradually over all the region at the same time.

3- There is a difference of about 5 hours between the occurrence of high tide in the north and the south of the gulf. This reveals that high water occurs in the north when low water exists in the south and vice versa.

4- Variations in width and depth of the gulf have great influences on the speed and direction of the current. Reflections and refractions of the tidal waves could be easily traced along the length of the gulf.

5- At high and low tides the tidal currents oftenly are weak every where in the gulf where eddies of different types of rotation are formed at different locations. These types of motion are very important in the marine environment. Whilst during the transient time strong currents flow along its main axis and divided into two branches nearly at its entrance in the vicinity of Ashrafi Island. These patterns agree well with current measurements recorded in that region (unpublished data).

6- The construction of current ellipses at selected locations in the gulf reflects the influence of the transverse motion which appears quite well in the southern part of the gulf, where the ratio between minor and major axis is significant.

7- More precise results and good representations for M2-tide and tidal current patterns have been obtained, which are in good agreement with observations. The spatial current distributions are very interesting and useful to predict a primitive pattern for the water circulation in the Gulf of Suez.

REFERENCES

Blondel, A., 1912. Sur la theorie des marees dans un canal. Appl. a mer Rouge. Ann. Fac. Toulouse, 3:151-207.

Chandon, E., 1930. Int. Hydrogr. Rev., 7: 176-77.

Defant, A., 1926. Gezeiten und Gezeitenstromungen in Roten Meer. Ann. Hydr. Mar. Met., Berlin, 54: 185-94.

Defant, A., 1961. Physical Oceanography, Oxford, Pergamon Press, Vol. 2: 598p.

Grace, S.F., 1930. The semidiurnal motion of the Red Sea. Mon. Not. R. Astr. Soc. Geophys. Suppl., 2: 273-96.

Hansen, W. 1956. Theorie zur Errechnung des Wasserstandes und der Stroemungen in Randmeeren nebst Anwendungen. Tellus No. 3.

Hansen, W., 1962. Hydrodynamical methods applied to oceanographic problems. Proc. of the Symposium on mathematical - hydrodynamical methods of physical oceanography. Mitt. Inst. Meeresk. Hamburg, No.1

Harris, R.A., 1904. Manual of Tides, Appendices, U.S. Coast and Geod. Surv. Rep. Part IV, 363-64.

Platzman, G.W., 1972. Two dimensional free oscillations in natural basins. J. Phy. Oceanogr. Vol. 2, No.2: 117-138.

Rady, M.A.,1992. Hydrodynamical numerical modelling of water movement in the Gulf of Suez. Ph.D. dissertation, Uni. du Quebec A'Rimouski, Canada, 188p.

Roberts, H.H. and S.P. Murray, 1984. Developing carbonate platforms: Southern Gulf of Suez, Northern Red Sea. Marine Geology, 59: 165-185.

Soliman, G.F., 1979. Application of the hydrodynamical equations to the circulation in the Red Sea. Ph.D. Thesis, Fac. Sci., Cairo Uni., 90 P.

Soliman, G.F. and M.A. Gerges, 1983. Effect of bottom topography on the tide in the Red Sea. Inter. Conf. on the Red Sea, Ghardaqa, Egypt, 1982. Bull. Inst. Oceanogr. & Fish., ARE. 8: 42-47.

Soliman, G.F.; A.M. Abdallah; F.M. Eid; S.H. Sharaf El-Din and I.A. Maiyza, 1993. Numerical investigation of M2-Tide in the Mediterranean as a closed basin. Bull. Inst. Oceanogr. & Fish., ARE. 19: 1-19.

Sterneck, R., 1927. Selbstaendige Gezeiten und Mitschwingen im Roten Meeres. Ann. Hydro. Mar. Mat., 55: 129-34.

Vercelli, F., 1925. Richerche di oceanographia fisia esequite della R. Nave AMMIRAGLIO MAGNAGHI (1923-1924), Part I, Correnti e maree. Ann. Idrog., 11: 1-188.